ACS OMEGA

http://pubs.acs.org/journal/acsodf

Article

Novel Vertical Flow Immunoassay with Au@PtNPs for Rapid, Ultrasensitive, and On-Site Diagnosis of Human Brucellosis

Jinhui Lu,[⊥] Chengcheng Li,[⊥] Enhui Zhang, Shuiping Hou, Ke Xiao, Xiaozhou Li, Ling Zhang, Zhen Wang, Chuangfu Chen, Chengyao Li,* and Tingting Li*

Cite This: *ACS Omega* 2023, 8, 29534−29542

Read Online

ACCESS | Metrics & More | Article Recommendations | Supporting Information

ABSTRACT: Brucellosis is an infectious zoonosis caused by *Brucella* with clinical symptoms of wavy fever, fatigue, and even invasion of tissues and organs in the whole body, posing a serious threat to public health around the world. Herein, a novel vertical flow immunoassay based on Au@Pt nanoparticles (Au@PtNPs-VFIA) was established for detection of *Brucella* IgG antibody in clinical serum samples. The testing card of Au@PtNPs-VFIA was manufactured by printing the purified *Brucella* LPS and goat antimouse IgG on the nitrocellulose membrane as the test-spot or control-spot, respectively. Au@PtNPs labeled with protein G (Au@PtNPs-prG) were concurrently employed as detection probes presenting visible spots and catalysts mimicking catalytic enzymes to catalyze the DAB substrate (H_2O_2 plus O-phenylenediamine) for deepening color development. The testing procedure of Au@PtNPs-VFIA takes 2−3 min, and the limit of detection (LOD) for *Brucella* antibody is 0.1 IU/mL, which is faster and more sensitive than that of Au@PtNP-based lateral flow immunoassay (Au@PtNPs-LFIA: 15 min and 1.56 IU/mL, respectively). By comparing with vertical flow immunoassay based on classic Au nanoparticles (AuNPs-VFIA), the Au@PtNPs-VFIA is 32 times or 16 times more sensitive with or without further development of DAB substrate catalysis. Au@PtNPs-VFIA did not react with the serum samples of Gram-negative bacterium infections but only weakly cross-reacted with diagnostic serum of *Y. enterocolitica* O9 infection. In detection of clinical samples, Au@PtNPs-VFIA was validated for possessing 98.33% sensitivity, 100% specificity, and 99.17% accuracy, which were comparable with or even better than those obtained by the Rose-Bengal plate agglutination test, serological agglutination test, AuNPs-VFIA, and Au@PtNPs-LFIA. Therefore, this newly developed Au@PtNPs-VFIA has potential for rapid, ultrasensitive, and on-site diagnosis of human Brucellosis in clinics.

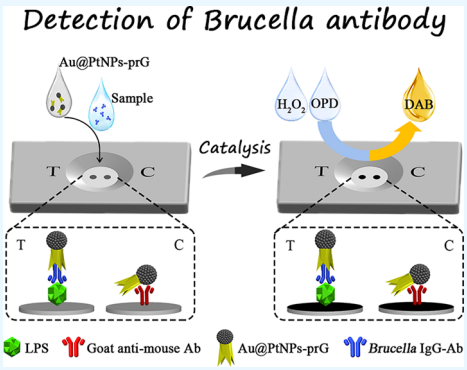

INTRODUCTION

Brucellosis is a serious and often neglected zoonosis caused by *Brucella* infection through contacting the contaminated animal and its products or air dusts.[1] Livestock such as cattle,[2] goats,[3] sheep,[4] camels,[5] and pigs[6] is the most common intermediate hosts of *Brucellae*, and humans, as the ultimate host, get sick through direct or indirect contact with infected animals or eating contaminated animal products.[7] Around the world, 500,000 people are diagnosed with *Brucella* infection every year.[8] In China, a total of 44,036 people were confirmed with brucellosis in 2019, with an incidence rate of 3.2513/100,000.[9] Human brucellosis has a long process of development and persistence and can eventually develop into chronic granulomatous diseases, which invade the central and peripheral nervous systems, as well as the musculoskeletal, skin systems, urogenital system, liver and gallbladder, cardiovascular, and gastrointestinal tract.[1] Although brucellosis is rarely fatal, it can cause patients' disability and inability to work. With its early fever characteristics, brucellosis cunningly disguise itself as a common febrile disease, such as cold. The early symptoms of patients with brucellosis are usually nonspecific symptoms that are not easy to distinguish from other febrile diseases and often to escape early diagnosis. Therefore, accurate and specific laboratory detection methods are urgently needed for differential diagnosis. Moreover, early and accurate diagnosis of human brucellosis is not only important for timely treatment of patients but also of great significance for prevention and control of brucellosis.

Currently, laboratory diagnostic methods for human *Brucella* infection mainly include three modalities with different principles, including bacterium culture and identification,[10,11] sero-diagnosis such as enzyme-linked immunosorbent assay (ELISA),[12] fluorescence polarization immunoassay (FPA),[13] serological agglutination test (SAT),[14] and Rose-bengal plate agglutination test (RBPT),[15] and molecular diagnosis.[16,17] The

Received: May 15, 2023
Accepted: July 18, 2023
Published: August 3, 2023

https://doi.org/10.1021/acsomega.3c03381
ACS Omega 2023, 8, 29534−29542

Brucella isolation is the gold standard for the diagnosis of brucellosis, but it requires strict laboratory and biosafety conditions. FPA and ELISA have high sensitivity, but with the drawbacks of expensive equipment, complex operation, time consumption, and professional laboratory technicians.[13,18] RBPT and SAT use the whole bacteria or the unpurified smooth lipopolysaccharides as antigens, which have low sensitivity and may cross-react with other Gram-negative bacteria.[19−21] In addition, SAT takes approximately 24 h. Molecular diagnosis, such as polymerase chain reaction (PCR), has high sensitivity and specificity for *Brucella* infection diagnosis and can accurately classify *Brucella* strains.[22,23] However, molecular diagnosis is time-consuming and requires expensive reagents, equipment, and professional laboratory technicians. Lateral flow immunoassay (LFIA) is widely reported in the rapid diagnosis of brucellosis because it is portable and easy to operate and does not need expensive instruments and professional laboratory personnel to interpret the results. An ultrasensitive dual-color rapid LFIA with gold nanoparticles was established for rapid serodiagnosis of brucellosis.[24] In addition, an LFIA based on colored latex microspheres was also developed for detection of *Brucella* infections.[25] In our previous study, we have established a digital LFIA for quantitative detection of *Brucella* IgG antibody based on time-resolved fluorescent microspheres.[26] All those studies strongly suggest that LFIA based on nanoparticles has unpredictable potential in the diagnosis of brucellosis.

Vertical flow immunoassay (VFIA) is different from LFIA, and its working principle is based on vertical filtration. In VFIA, the nitrocellulose (NC) membrane is used as the solid support of antigen or antibody, and the nanoparticle conjugate is used as the detection probe, respectively, and the complete specific immune affinity reaction is carried out with the filterability of the NC membrane. Compared with LFIA, VFIA has the advantages of shorter detection time and no hook effect. However, the nanodetection probes of VFIA exist in the solution, so that they can percolate through the NC membrane. Currently, VFIA has been used in the detection of food safety,[27] inflammatory factors,[28] and microorganisms,[29,30] presenting satisfactory detection performance. However, the assay's sensitivity needs to be improved.

Nanozymes are nanomaterials with enzyme-like activity. Compared with natural enzymes, nanozymes have been widely used in biomedical research due to their advantages of low cost, simple preparation, and higher stability.[31] As the earliest nanozyme, the Fe_3O_4 nanozyme has been applied in tumor therapy due to its reactive oxygen species generation ability and tumor cell killing ability.[32] Recently, a novel peptide-templated manganese dioxide nanozyme (PNzyme/MnO2) combined the thrombolytic activity of functional peptides with the reactive oxygen species scavenging ability of nanozymes for the treatment of ischemic stroke.[33] In addition to medical treatment, nanozymes have also been applied to replace natural enzymes for the establishment of diagnostic methods.[34−38] According to reports, nanozymes containing Group-VIII metal elements (Pt > Ir > Pd > Ru > Rh) can replace catalase to catalyze the decomposition of H_2O_2 to produce O_2.[39] Au@PtNPs are a kind of nanozyme composited by the combination of Au and Pt ions, which have the function of catalytic enzymes such as catalase.[34] Based on the catalytic characteristics, Au@PtNPs have been used for detection probes visible on test-line as well as for further color development of catalyzing substrate reaction in LFIA for the detection of peroxidase-containing samples,[35] HIV p24,[36] *Escherichia coli* O157:H7[37] and prostate-specific antigen.[38] In our laboratory, Au@PtNPs have been proven to be a nanozyme with stronger catalytic activity than horseradish peroxidase (HRP) and have been employed as a detection probe for diagnosis of SARS-CoV-2 infection.[40,41] However as far as we know, Au@PtNPs have not been applied in VFIA.

The aim of this research is to apply Au@PtNPs in a traditional VFIA and to improve the sensitivity of VFIA based on catalyzing the DAB substrate (H_2O_2 plus OPD) by Au@PtNPs. Herein, we first develop a novel testing card of VFIA based on Au@PtNPs (Au@PtNPs-VFIA) for rapid, ultrasensitive, and on-site detection of *Brucella* IgG antibody in clinical serum samples. In this Au@PtNPs-VFIA, Au@PtNPs labeled with streptococcus protein G (prG) are used as detection probes, the purified *Brucella* LPS is employed as coating antigen on the test-spot of NC membrane, and goat anti-mouse IgG is immobilized on the control-spot as a quality control, respectively. When the DAB substrate is added to the detection area after the filtration reaction, the sensitivity of Au@PtNPs-VFIA is significantly increased.

RESULTS AND DISCUSSION

Working Principle of Au@PtNPs-VFIA and Au@PtNPs-LFIA. The testing card of Au@PtNPs-VFIA is assembled by three parts of the NC filter membrane, absorbent paper, and plastic shell (Figure 1A,B). As shown in Figure 1C, when a serum sample containing anti-*Brucella* antibodies is added on the detection area of the testing card, the anti-*Brucella* IgG antibodies are captured by the precoated *Brucella* LPS on the

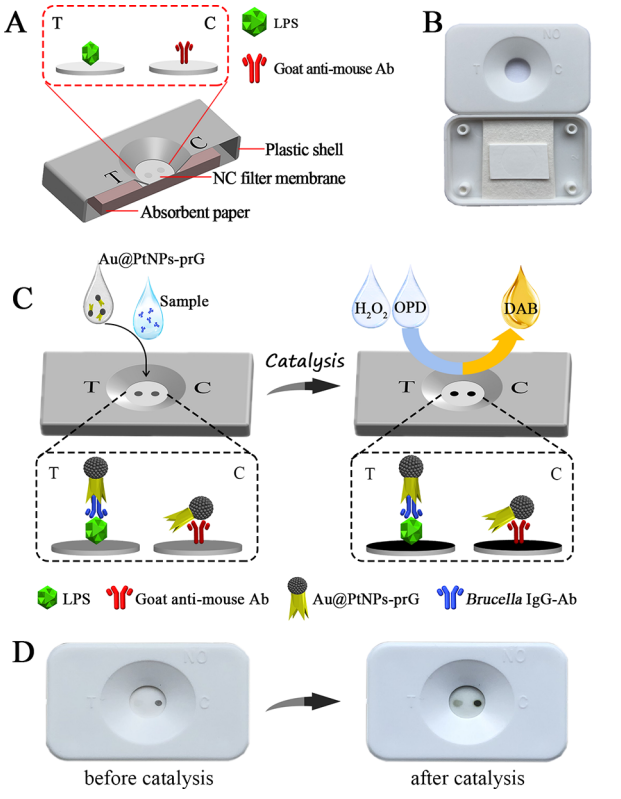

Figure 1. Schematic diagram of Au@PtNPs-VFIA. (A) Model of the testing card. (B) Assembly of the testing card. (C) Schematic diagram of Au@PtNPs-VFIA. (D) Before or after catalysis of Au@PtNPs-VFIA for reading results.

https://doi.org/10.1021/acsomega.3c03381
ACS Omega 2023, 8, 29534−29542

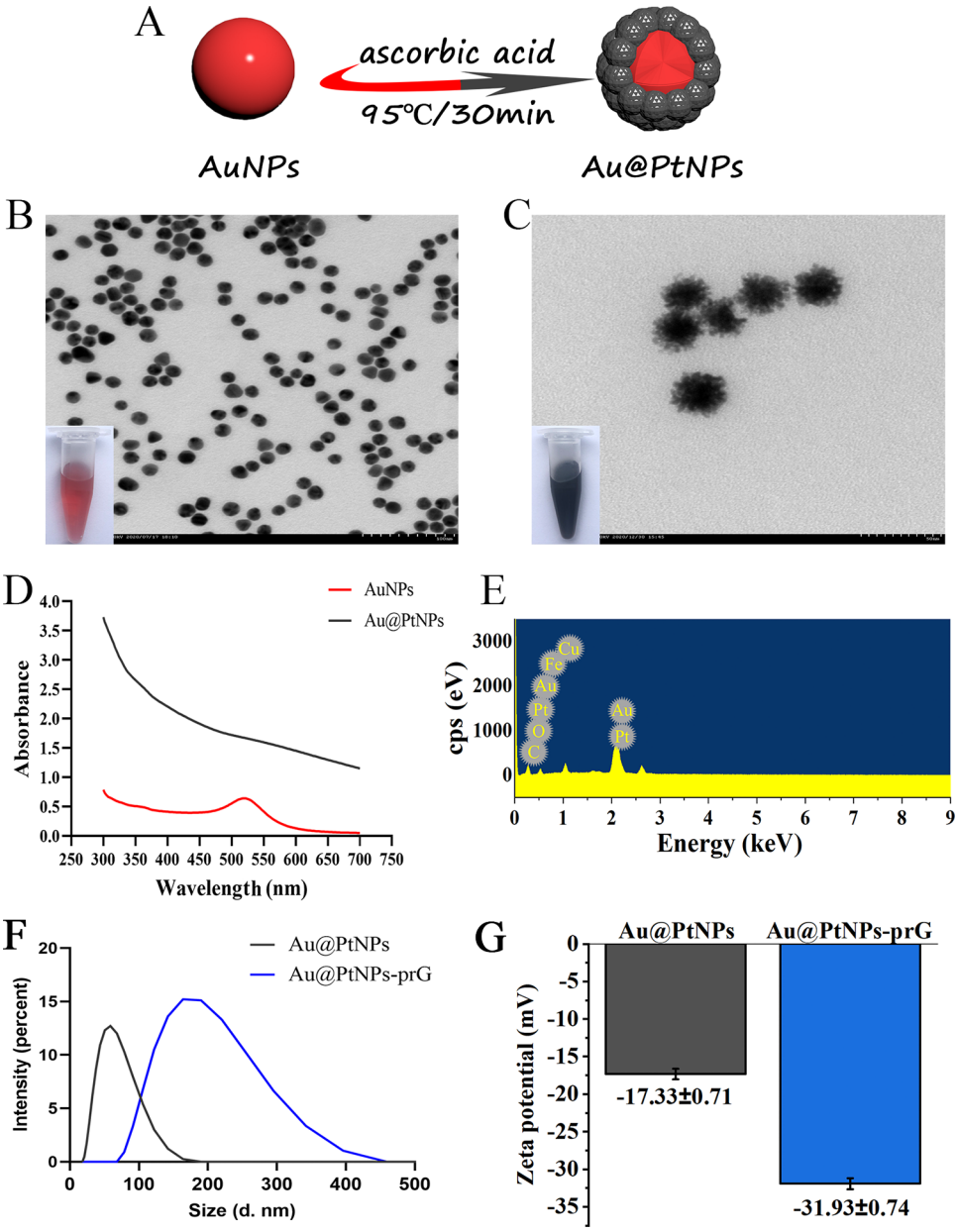

Figure 2. Characterization of Au@PtNPs and Au@PtNPs-prG. (A) Synthesis procedure for Au@PtNPs. (B) Au seed colloidal solution and its transmission electron microscopy (TEM) image. (C) Au@PtNP colloidal solution and its TEM image. (D) Ultraviolet-visible (UV−vis) spectrum scanning of Au seeds and Au@PtNPs. (E) EDX spectroscopy of Au@PtNPs. (F) Hydrodynamic diameters of Au@PtNPs and Au@PtNPs-prG. (G) Zeta potentials of Au@PtNPs and Au@PtNPs-prG.

T-spot to form LPS-IgG complexes. Then, the detection probes of Au@PtNPs-prG are dropped on the detection area, the Au@PtNPs-prG bind to LPS-IgG complexes via a high-affinity reaction between IgG and prG, showing a black spot on T-spot; meanwhile, Au@PtNPs-prG bind to the precoated goat antimouse IgG and appear to a black spot on the C-spot of the testing card. None bound antibodies, extra Au@PtNPs-prG conjugates, and other residues are washed through NC membrane filtration with PBS buffer. Finally, after the DAB substrate (H_2O_2 plus OPD chromogen) is loaded on the testing card with the visible spot, Au@PtNPs-prG play a role as catalysts instead of catalytic enzymes (for instance, peroxidase) to catalyze H_2O_2 and to release hydroxyl radicals. By oxidation between OPD and hydroxyl radicals, the precipitated diaminoazobenzene (DAB) is generated for gradually deepening the black spots on the T-spot and C-spot, which significantly improve the sensitivity of assay (Figure 1D).

The working principle of Au@PtNPs-LFIA is as follows (Figure S1A,B): When a serum sample containing anti-*Brucella* antibody is dropped on the sample pad, the running buffer surrounds the sample and flows forward, and the anti-*Brucella* IgG antibodies are captured by the Au@PtNPs-prG spraying on the conjugate pad to form Au@PtNPs-prG-IgG complexes. Then, when the Au@PtNPs-prG-IgG complexes flow to the T-line, the specific Au@PtNPs-prG-IgG complexes are captured by the precoated *Brucella* LPS on the T-line to form Au@PtNPs-prG-IgG-LPS complexes, showing a black line on the T-line. Extra Au@PtNPs-prG complexes continue to flow forward and bind to the precoated goat antimouse IgG on the C-line, forming a black line as a control. When the black

https://doi.org/10.1021/acsomega.3c03381
ACS Omega 2023, 8, 29534−29542

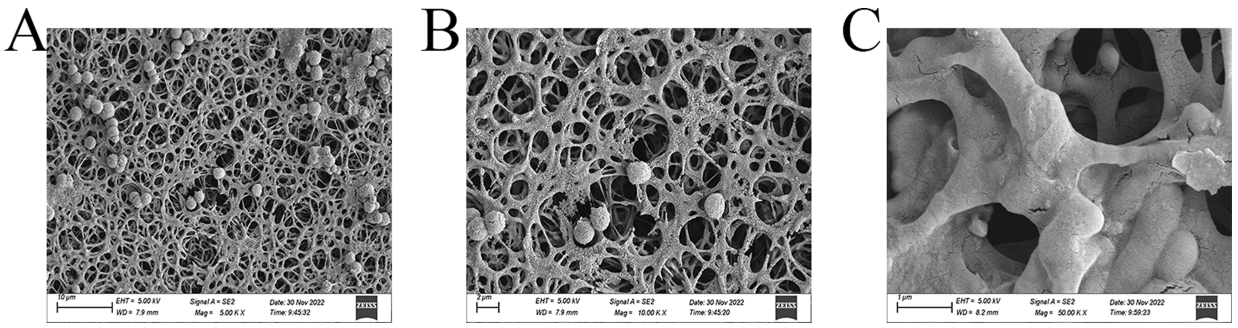

Figure 3. SEM image of the NC filter membrane. (A) 5.00 kx magnification. (B) 10.00 kx magnification. (C) 50.00 kx magnification.

line appears on both the T-line and the C-line, it indicates a positive result; when only a black line appears on the C-line, it indicates a negative result (Figure S1C).

Characterization of Au@PtNPs, Au@PtNPs-prG, PtNPs, and NC Filter Membrane. By a two-step hydrothermal method (Figure 2A), eight kinds of Au@PtNPs were successfully synthesized according to various amounts of Au seeds (Figure S2A, Table S1). Au seeds were spherical with a diameter of about 10 nm (Figures 2B and S2B). With the increase of chloroplatinic acid hexahydrate, the particle size of Au@PtNPs was gradually enlarged, the spike structures on the surface became larger, and the appearance color changed from light red to platinum black (Figure S2A,B). The absorption peak of Au seeds at 525 nm was gradually eliminated from Au@PtNPs-1 to Au@PtNPs-8, while Au@PtNPs-7 happened to have no absorption peak at 525 nm at all (Figure S2C). The catalytic dynamic curves showed that Au@PtNPs-7 had stronger catalytic power (Figure S3). Under the above conditions, Au@PtNPs-7 (designated as Au@PtNPs) was selected to prepare Au@PtNPs-prG conjugates as detection probes.

As shown in Figure 2C, the average particle size of Au@PtNPs is 50 nm. The color of Au seed solution is red, and its unique characteristic is the absorption peak at 525 nm (Figure 2B,D). The significant differences between Au seeds and Au@PtNPs are the spike structure on the Au@PtNPs surface in morphology and the absence of an absorption peak at 525 nm (Figure 2B−D), indicating that all particle surfaces of Au seeds are decorated with saturated PtNPs. The energy-dispersive X-ray (EDX) spectroscopy observations confirm that the weight percentage and atomic percentage of Au ions are 30.65 and 9.51% in Au@PtNPs, whereas the weight percentage and atomic percentage of Pt ions are 37.77 and 11.83%, respectively (Figures 2E and S4). After Au@PtNPs are labeled with prG, the hydrodynamic diameters increase significantly from 54.70 ± 1.30 to 170.23 ± 2.91 nm (Figure 2F). Meanwhile, Au@PtNPs-prG are stable due to the sufficiently higher value of zeta potential (−31.93 ± 0.74 mV) by comparing with Au@PtNPs (−17.33 ± 0.71 mV) (Figure 2G).

The PtNP solution is light platinum black with no absorption peak at 525 nm (Figure S5A). The surface of PtNPs is filled with spikes, resembling a sea urchin in shape (Figure S5B). Compared with the average 50 nm particle size of Au@PtNPs, the average particle size of PtNPs is smaller, at 30 nm (Figure S5B).

To ensure that free Au@PtNPs-prG can be easily filtered through the NC membrane to absorbent paper, the pore size of the NC filter membrane has been measured by SEM. The SEM image shows that the NC filter membrane possesses approximately 0.8 μm size pores (Figure 3), which are large enough to enable free Au@PtNPs-prG to pass through.

Optimization of Au@PtNPs-VFIA, PtNPs-VFIA, and AuNPs-VFIA. Six key elements for Au@PtNPs-VFIA were optimized (Table S2), of which the optimal concentration of tetronic 1307 was determined for 2% and gave the clean background in the detection area of the testing card (Figure S6). When the volume of Au@PtNPs-prG was 4 μL (Figure S7) and the concentration of *Brucella* LPS was 160,000 EU/mL (Figure S8), the Au@PtNPs-VFIA presented the highest positive signal with no background. The C-spot reached a plateau of color development when the concentration of goat antimouse IgG was at 0.25 mg/mL (Figure S9). When the concentration of H_2O_2 was 6% and the concentration of OPD was 0.1 M, the T-spot reached a plateau in 2 min and the background of the detection area was clean (Figure 4).

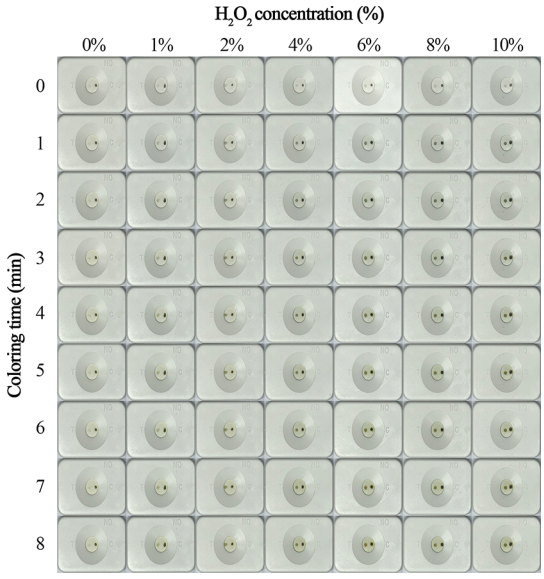

Figure 4. Optimization of H_2O_2 concentration and color-developing time in the DAB substrate (H_2O_2 plus OPD).

In parallel, PtNPs-VFIA and AuNPs-VFIA were optimized and used as control assays. AuNPs were evenly dispersed and had an absorption peak at nearly 528 nm, while the colloidal solution was wine red (Figure S10A,B). The positive and negative results of AuNPs-VFIA are shown in Figure S10C.

Performance Comparison among Au@PtNPs-VFIA, PtNPs-VFIA, AuNPs-VFIA, and Au@PtNPs-LFIA. The sensitivity of Au@PtNPs-VFIA was measured for detecting different concentrations of standard brucellosis-positive serum.

https://doi.org/10.1021/acsomega.3c03381
ACS Omega 2023, 8, 29534−29542

A series of concentrations from 200 IU/mL to 0.01 IU/mL of standard brucellosis-positive serum were added on the detection area of the testing card. Before catalysis of the DAB substrate, a weak black T-spot was observed on the detection area even when the concentration of *Brucella* antibody was as low as 1.56 IU/mL (Figure 5A), which was

Figure 5. Sensitivity of Au@PtNPs-VFIA before and after catalysis. (A) Before catalysis. (B) After catalysis.

lower than the LOD (12.5 IU/mL) of PtNPs-VFIA before catalysis (Figure S11A) and the LOD (3.13 IU/mL) of AuNPs-VFIA (Figure S12). After adding the DAB substrate (H_2O_2 + OPD), the black T-spots between serum samples with 0.1 and 0.05 IU/mL became more clear (Figure 5B). The LOD of Au@PtNPs-VFIA was 0.1 IU/mL, of which the detection sensitivity was increased 16 times than before substrate catalysis. By comparing with control assays, the sensitivity of Au@PtNPs-VFIA was 16 times higher than that of PtNPs-VFIA after catalysis (LOD: 1.56 IU/mL) (Figure S11B) and 32 times higher than that of AuNPs-VFIA, respectively. The LOD of Au@PtNPs-VFIA at both before and after catalysis is much lower than that of PtNPs-VFIA, indicating that Au@PtNPs have better than PtNPs as a detection probe. Before catalysis, the LOD of PtNPs-VFIA (12.5 IU/mL) is significantly higher than that of AuNPs-VFIA (3.13 IU/mL), meaning that the performance of PtNPs is far inferior to that of AuNPs.

Meanwhile, the detection sensitivity of Au@PtNPs-LFIA was evaluated and compared with Au@PtNPs-VFIA. The LOD of Au@PtNPs-LFIA was 1.56 IU/mL (Figure S13), equal to that of Au@PtNPs-VFIA before catalysis (1.56 IU/mL) and 16 times higher than that of Au@PtNPs-VFIA after catalysis (0.1 IU/mL). The entire reaction time of Au@PtNPs-LFIA was 15 min, significantly longer than that of Au@PtNPs-VFIA (2−3 min). Therefore, after additions of sample and reagent, Au@PtNPs-VFIA had superior ability to quickly bind and wash reactants compared to Au@PtNPs-LFIA. In addition, compared with Au@PtNPs-LFIA, the results of Au@PtNPs-VFIA were not affected by the proportion of antigens and antibodies in the samples. In Au@PtNPs-VFIA, nonspecific antibodies were eliminated through vertical filtration in the first step of sample addition, while only specific antibodies were captured by LPS immobilized on the NC filter membrane. The above results suggested that the established Au@PtNPs-VFIA had higher sensitivity, shorter reaction time, and no hook effect for the detection of *Brucella* antibodies.

To evaluate the specificity of Au@PtNP-VFIA, a panel of clinical serum samples from Gram-negative bacterium (*Serratia marcescens*, *Stenotrophomonas maltophilia*, *Proteus mirabilis*, *Pseudomonas aeruginosa*, *Escherichia coli*, *klebsiella pneumoniae*, *Acinetobacter baumannii*) infected patients, *E. coli* O157 and *Y. enterocolitica* O9 diagnostic sera were tested in comparison with 0.2 IU/mL *Brucella* IgG antibody control (Figure 6). No

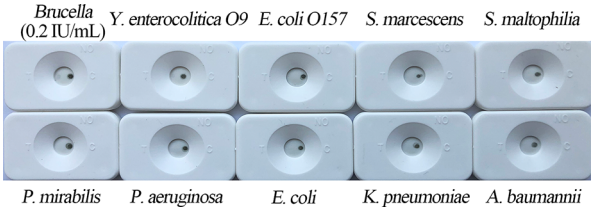

Figure 6. Cross-reactivity of Au@PtNPs-VFIA with serum samples from other bacterium-infected patients.

cross-reactivity was found except for a weak black T-spot from *Y. enterocolitica* O9 diagnostic serum. LPS is composed of lipid A, core oligosaccharide, and O-antigen, of which O-antigen is the most important antigen component.[42] The structure of O-antigens is different among Gram-negative bacteria; for example, there are 46 main O-serogroups in Salmonella and more than 180 recognized O-serotypes in *E. coli*.[43−45] *Brucella* LPS has been reported for having cross-reacting epitopes with *E. coli* O157 and *Y. enterocolitica* O9 antigens.[46] However, in our previous study,[26] the purified *Brucella* LPS has confirmed that it only has a weak cross-reaction with the epitope of *Y. enterocolitica* O9 antigen. Herein, the detection of Au@PtNPs-VFIA was only weakly interfered by *Y. enterocolitica* O9 diagnostic antibodies and not interfered by other serum samples of Gram-negative bacterium or *E. coli* O157 diagnostic antibodies. The results suggested that Au@PtNPs-VFIA had satisfactory specificity.

The intrabatch and interbatch stabilities of Au@PtNPs-VFIA testing cards were evaluated uninterruptedly for two weeks. Three intrabatch testing cards and two interbatch testing cards showed satisfactory stability in *Brucella* antibody (0.2 IU/mL) detection (Figure S14), suggesting that the testing cards had stable performance for at least two weeks stored at room temperature.

Detection of *Brucella* IgG Antibody in Clinical Serum Samples. By using optimized Au@PtNPs-VFIA, 60 brucellosis patients' and 60 healthy people's serum samples were tested in comparison with AuNPs-VFIA, RBPT, and SAT. The results are presented in Table 1, and the details of 60 brucellosis patients' serum samples were provided in Table S3. Among 60 brucellosis patients' samples, 59 (98.33%) were all detected positive by Au@PtNPs-VFIA, AuNPs-VFIA, or AuNPs-LFIA, while 57 (95%) were positive by RBPT and 55 (91.67%) were positive by SAT, respectively. In terms of specificity, of 60 healthy individuals' samples, all were detected negative by all methods. The accuracy of Au@PtNPs-VFIA, AuNPs-VFIA, and Au@PtNPs-LFIA was consistent with 99.17% (*Kappa* value of 0.98, $P < 0.05$), whiles RBPT was 97.5% (*Kappa* value of 0.95, $P < 0.05$) and SAT was 95.83% (*Kappa* value of 0.91, $P < 0.05$), respectively. Evidently, the sensitivity, specificity, and accuracy of Au@PtNPs-VFIA were comparable with or even better than those obtained by control methods, demonstrating that Au@PtNPs-VFIA was applicable to the detection of *Brucella* IgG antibody in clinical serum samples.

https://doi.org/10.1021/acsomega.3c03381
ACS Omega 2023, 8, 29534−29542

Table 1. Detection of *Brucella* Antibody in Clinical Samples from Brucellosis Patients by RBPT, SAT, Au@PtNPs-VFIA, AuNPs-VFIA, and Au@PtNPs-LFIA[a]

	RBPT		SAT		Au@PtNPs-VFIA		AuNPs-VFIA		Au@PtNPs-LFIA	
	+	−	+	−	+	−	+	−	+	−
negative group (n = 60)	0	60	0	60	0	60	0	60	0	60
positive group (n = 60)	57	3	55	5	59	1	59	1	59	1
sensitivity (%)	95 (57/60)		91.67 (55/60)		98.33 (59/60)		98.33 (59/60)		98.33 (59/60)	
specificity (%)	100 (60/60)		100 (60/60)		100 (60/60)		100 (60/60)		100 (60/60)	
Kappa value*	0.95		0.91		0.98		0.98		0.98	
accuracy (%)	97.5 (117/120)		95.83 (115/120)		99.17 (119/120)		99.17 (119/120)		99.17 (119/120)	

[a]*P < 0.05.

Table 2. Comparison between Au@PtNPs-VFIA and Reported Flow Immunoassays (FIA) with LPS Antigen[a]

FIA type	type of labels	coating antigen	limit of detection	detection time	references
vertical	Au@PtNPs-prG	LPS	0.1 IU/mL	2−3 min	this study
vertical	PtNPs-prG	LPS	1.56 IU/mL	2−3 min	this study
vertical	AuNPs-prG	LPS	3.13 IU/mL	2−3 min	this study
lateral	Au@PtNPs-prG	LPS	1.56 IU/mL	15 min	this study
vertical	GNPs-SPA	LPS	4 IU/mL	3−5 min	30
vertical	flower-like GNPs-SPA	LPS	2 IU/mL	2−3 min	47
vertical	AuNPs-SPA	LPS	4 IU/mL	5−6 min	48
lateral	GNDs-SPA	LPS	0.04 IU/mL	3 min	24
lateral	SiNPs-SPA	LPS	0.01 IU/mL	15 min	49
lateral	EuNPs-prG	LPS	0.3 IU/mL	15 min	26

[a]Abbreviations: GNPs, gold nanoparticles; GNDs, durian-like gold nanoparticles; SiNPs, silica nanoparticles; EuNPs, europium nanoparticles; SPA, staphylococcal protein A.

Compared with else immunoassays established in this study and previously established flow immunoassays with *Brucella* LPS as coating antigen (Table 2), Au@PtNPs-VFIA had obvious advantages in sensitivity (LOD 0.1 IU/mL) and detection time (2−3 min).

CONCLUSIONS

In this study, we developed a vertical flow immunoassay with catalytic enzyme functional Au@PtNPs, which was successfully applied for rapid testing of *Brucella* IgG antibody. Au@PtNPs-VFIA takes only 2−3 min for testing, and its LOD is 0.1 IU/mL, which is about 32 times or 16 times more sensitive to that of AuNPs-VFIA or Au@PtNPs-LFIA, respectively. Au@PtNPs-VFIA was demonstrated to possess 98.33% sensitivity, 100% specificity, and 99.17% accuracy for the detection of *Brucella* IgG antibody from clinical serum samples. In principle, Au@PtNPs-VFIA could be further applied for the diagnosis of brucellosis in livestock. Compared with Au@PtNPs-LFIA, the Au@PtNPs-VFIA has the advantages of higher sensitivity, shorter detection time, and no hook effect. Meanwhile, the testing card is small and portable, making it more suitable for on-site diagnosis. Overall, this work showcased the potential value of Au@PtNPs as an immune detection probe and mimic peroxidase in immunoassays, and Au@PtNPs-VFIA could be a novel model for rapid, ultrasensitive, and on-site diagnosis of human Brucellosis.

EXPERIMENTAL SECTION

Reagents, Materials, and Apparatus. $HAuCl_4{\cdot}3H_2O$, bovine serum albumin (BSA), ascorbic acid, sodium citrate, trehalose, sucrose, K_2CO_3, 30% (w/w) H_2O_2, and O-phenylenediamine (OPD) were obtained from Sigma-Aldrich (Shanghai, China). Chloroplatinic acid hexahydrate was purchased from BBI life science (Shanghai, China). Tetronic 1307 was obtained from Shanghai Yuanye Biological Technology Co., Ltd. (Shanghai, China). Other reagents were purchased from Sigma-Aldrich (Shanghai, China) and all the reagents used in this research were of analytical grade. Streptococcus protein G (prG) was purchased from Hangzhou Niulong Biological Technology Co., Ltd. (Hangzhou, China). *Brucella abortus 2308* lipopolysaccharide (LPS) was obtained from the Key Laboratory of Animal Disease Prevention, College of Animal Science and Technology, Shihezi University, Xinjiang, China, and further purified in our laboratory.[26] Goat antimouse IgG antibody was obtained from Beijing Bersee Technology Co., Ltd. (BeiJing, China). SAT and RBPT test kits were provided by Qingdao Zhongchuang Huike Biotechnology Co., Ltd. (Qingdao, China). Standard brucellosis-positive serum (4000 IU/mL) was obtained from the China Institute of Veterinary Drug Control (Beijing, China).

The nitrocellulose (NC) filter membrane (CLW-0400, 0.8 μm pore size) was purchased from Advanced Microdevices Pvt. Ltd. (India). The absorbent pad and plastic shell were obtained from Shanghai Jieyi Biotechnology Co., Ltd. (Shanghai, China).

Ultrapure water with 18.2 MΩ/cm resistivity was produced by a Milli-Q Ultra-Pure System (Millipore, USA). An X-ray energy spectrometer (XFlash 6130, Bruker, Germany), a transmission electron microscope (TEM, Philips, Holland), and a nanometer particle size potentiometer (Zetasizer Nano ZS90, Malvern panalytical, England) were used for analyzing the component, characteristic, or particle size of nanoparticles. A scanning electron microscope (SEM, ZEISS, Germany) was used for characterizing the NC filter membrane. Shell pressing apparatus (Shanghai Jinbiao Biotechnology Co., Ltd., Shanghai, China) was used for assembling the testing card.

Clinical Samples. In total, 60 serum samples of brucellosis patients were provided by Guangzhou Center for Disease

https://doi.org/10.1021/acsomega.3c03381
ACS Omega 2023, 8, 29534−29542

Control and Prevention. All *Brucella*-infected patients were confirmed based on the Health Industry Standards of the People's Republic of China (WS269-2019, Diagnostic criteria for brucellosis). Sixty serum samples of healthy people and seven serum samples of Gram-negative bacterium-infected patients were collected from Guangdong Second Hospital of Traditional Chinese Medicine, China. In addition, *E. coli* O157 and *Yersinia (Y.) enterocolitica* O9 diagnostic antisera (Tianjin Biochip Technology Co., Ltd., China) were employed to test the cross-reactivity of established VFIA.

Preparation of Au@PtNPs-prG and PtNPs-prG. In this experiment, Au@PtNPs were synthesized by the hydrothermal method and optimized by adjusting the component ratio (Table S1). Preparation and evaluation of Au@PtNPs catalytic performance are partly available in supplementary materials. After optimization of the component ratio, the synthesis procedure of Au@PtNPs was as follows: First, Au nanoparticles were synthesized and used as seeds for subsequent synthesis. Briefly, 0.01% $HAuCl_4{\cdot}3H_2O$ and 0.04% sodium citrate were dissolved in 100 mL of ultrapure water and heated to 100 °C for 30 min. Second, 8.60 mL of Au seeds and 0.60 mL of chloroplatinic acid hexahydrate (20 mM) were mixed and heated to 95 °C for 5 min, and then 0.8 mL of ascorbic acid (20 mM) were added drop by drop and incubated at 95 °C for 30 min. Meanwhile, following the above optimum synthesis process, Pt nanoparticles (PtNPs) were synthesized as a control by replacing Au seeds with ultrapure water. Finally, the synthesized Au@PtNPs and PtNPs were characterized by a X-ray energy spectrometer, TEM, and nanometer particle size potentiometer, respectively.

The Au@PtNPs-prG or PtNPs-prG were prepared as follow: 1 mL of Au@PtNPs or PtNPs was adjusted to pH 5.5−6.0 using 0.2 M K_2CO_3, and then 20 μg of prG was added, mixed, and incubated for 20 min. After incubation, 100 μL of 10% BSA was added, mixed, and blocked for 20 min. The conjugates were then centrifuged at 10,000 g for 15 min and re-suspended in 0.1 mL of preservation solution (5% trehalose, 5% sucrose, 1% BSA, 10 mM Tris−HCl, pH 7.4), and stored at 4 °C.

Assembly of Testing Card of Au@PtNPs-VFIA and Au@PtNPs-LFIA. The testing card of Au@PtNPs-VFIA was composed of three parts, including the NC filter membrane, absorbent paper, and plastic shell (Figure 1A). Two separate detection points on NC membrane were coated with *Brucella* LPS as the test-spot (T-spot) or goat anti-mouse IgG as the control-spot (C-spot), respectively. To obtain the ideal performance of the testing card, the following elements were optimized for the concentration, volume, or time of surfactant, Au@PtNPs-prG, *Brucella* LPS, goat anti-mouse IgG, H_2O_2 and color development. Two additional testing cards of vertical flow immunoassay based on Pt nanoparticles (PtNPs-VFIA) or classic Au nanoparticles (AuNPs-VFIA) was prepared in the supplementary materials and employed as control assays respectively, sharing the same assembly processes with Au@PtNPs-VFIA. The assembly of the Au@PtNPs-LFIA testing card was described in the supplementary materials (Figure S1A, S1B).

Operation and Performance of Au@PtNPs-VFIA, PtNPs-VFIA, AuNPs-VFIA, and Au@PtNPs-LFIA. The operation procedure of Au@PtNPs-VFIA is optimized as following: Firstly, 10 μL of sample is mixed with 90 μL of running buffer and added on the detection area. Then, 100 μL of running buffer containing Au@PtNPs-prG is added to the detection area. Immediately, 100 μL of running buffer is added to clean the detection area. Finally, 50 μL of DAB substrate (H_2O_2 plus OPD) is added, and the result is observed visually in 2 min. The operation procedure of PtNPs-VFIA is consistent with Au@PtNPs-VFIA, and the operation procedure of AuNPs-VFIA is the same as Au@PtNPs-VFIA, but no OPD chromogen is needed.

The operation procedure of Au@PtNPs-LFIA is as follows: Firstly, 10 μL of sample is dropped on sample pad. Then, 80 μL of running buffer is dropped on the sample pad, and the result is observed visually in 15 min.

Standard brucellosis-positive serum was diluted from 200 IU/mL to 0.01 IU/mL by continuous 1:2 dilution to evaluate the sensitivities of Au@PtNPs-VFIA, PtNPs-VFIA, AuNPs-VFIA and Au@PtNPs-LFIA. Seven Gram-negative bacterium infected patients' serum samples and two *E. coli* O157 and *Y. enterocolitica* O9 diagnostic sera were employed to evaluate the specificity of Au@PtNPs-VFIA.

Ethical Statement. Clinical samples were routinely collected from Guangzhou Center for Disease Control and Prevention, or Guangdong Second Hospital of Traditional Chinese Medicine in China. All subjects in this research signed the informed consent form for the investigation. This research was reviewed and approved by Southern Medical University (SMU) Medical Ethics Committee (permit numbers: NFYY-2009-23).

■ ASSOCIATED CONTENT

Supporting Information

The Supporting Information is available free of charge at https://pubs.acs.org/doi/10.1021/acsomega.3c03381.

Methods, characterization, and catalytic performance of Au@PtNPs, optimal elements of Au@PtNPs-VFIA, schematic diagram and sensitivity of Au@PtNPs-LFIA, sensitivity of AuNPs-VFIA, sensitivity of PtNPs-VFIA, stability of Au@PtNPs-VFIA, and detection results of serum samples from 60 brucellosis patients (PDF)

■ AUTHOR INFORMATION

Corresponding Authors

Chengyao Li − *Department of Transfusion Medicine, School of Laboratory Medicine and Biotechnology, Southern Medical University, Guangzhou 510515, China*; Email: chengyaoli@hotmail.com

Tingting Li − *Department of Transfusion Medicine, School of Laboratory Medicine and Biotechnology, Southern Medical University, Guangzhou 510515, China*; orcid.org/0000-0001-5727-2179; Email: apple-ting-007@163.com

Authors

Jinhui Lu − *Department of Transfusion Medicine, School of Laboratory Medicine and Biotechnology, Southern Medical University, Guangzhou 510515, China*

Chengcheng Li − *Department of Transfusion Medicine, School of Laboratory Medicine and Biotechnology, Southern Medical University, Guangzhou 510515, China*

Enhui Zhang − *Department of Transfusion Medicine, School of Laboratory Medicine and Biotechnology, Southern Medical University, Guangzhou 510515, China*

Shuiping Hou − *Department of Transfusion Medicine, School of Laboratory Medicine and Biotechnology, Southern Medical University, Guangzhou 510515, China; Microbiological*

https://doi.org/10.1021/acsomega.3c03381
ACS Omega 2023, 8, 29534−29542

Laboratory, Guangzhou Center for Disease Control and Prevention, Guangzhou 510440, China

Ke Xiao − *Department of laboratory Medicine, Guangdong Second Traditional Chinese Medicine Hospital, Guangzhou 510095, China*

Xiaozhou Li − *Department of Transfusion Medicine, School of Laboratory Medicine and Biotechnology, Southern Medical University, Guangzhou 510515, China*

Ling Zhang − *Department of Transfusion Medicine, School of Laboratory Medicine and Biotechnology, Southern Medical University, Guangzhou 510515, China*

Zhen Wang − *Animal Science and Technology College, Shihezi University, Shihezi 832002 Xinjiang, China*

Chuangfu Chen − *Animal Science and Technology College, Shihezi University, Shihezi 832002 Xinjiang, China*

Complete contact information is available at: https://pubs.acs.org/10.1021/acsomega.3c03381

Author Contributions

⊥J.H.L. and C.C.L. contributed equally to this work. J.H.L. and C.C.L. participated in the study design, analysis of data, and writing of the manuscript. E.H.Z.: Experimental operation, formal analysis, and methodology. S.P.H.: Methodology and resources. K.X.: Methodology and resources. X.Z.L.: Experimental operation. L.Z.: Formal analysis and methodology. Z.W.: Methodology and resources. C.F.C.: Methodology and resources. C.Y.L.: Conceptualization, funding acquisition, methodology, supervision, and writing − review & editing. T.T.L.: Conceptualization, data curation, formal analysis, funding acquisition, methodology, supervision, and writing − review & editing.

Notes

The authors declare no competing financial interest.

■ ACKNOWLEDGMENTS

This work was supported by the grants from the Guangdong Natural Science Foundation Outstanding Youth Project (No. 2022B1515020050) and Provincial key laboratory of immune regulation and immunotherapy (No. 2022B1212010009).

■ REFERENCES

(1) Franco, M. P.; Mulder, M.; Gilman, R. H.; Smits, H. L. Human Brucellosis. *Lancet Infect. Dis.* **2007**, *7*, 775−786.

(2) Spicic, S.; Zdelar-Tuk, M.; Ponsart, C.; Hendriksen, R. S.; Reil, I.; Girault, G.; Leekitcharoenphon, P.; Rukavina, V.; Rubin, M.; Freddi, L.; Duvnjak, S. New Brucella Variant Isolated from Croatian Cattle. *BMC Vet. Res.* **2021**, *17*, 126.

(3) Bodenham, R. F.; Mazeri, S.; Cleaveland, S.; Crump, J. A.; Fasina, F. O.; de Glanville, W. A.; Haydon, D. T.; Kazwala, R. R.; Kibona, T. J.; Maro, V. P.; Maze, M. J.; Mmbaga, B. T.; Mtui-Malamsha, N. J.; Shirima, G. M.; Swai, E. S.; Thomas, K. M.; Barend, B. M.; Halliday, J. E. B. Latent Class Evaluation of the Performance of Serological Tests for Exposure to Brucella Spp. In Cattle, Sheep, and Goats in Tanzania. *PLoS Neglected Trop. Dis.* **2021**, *15*, No. e0009630.

(4) Dougas, G.; Katsiolis, A.; Linou, M.; Kostoulas, P.; Billinis, C. Modelling Human Brucellosis Based on Infection Rate and Vaccination Coverage of Sheep and Goats. *Pathogens* **2022**, *11*, 167.

(5) Muturi, M.; Akoko, J.; Nthiwa, D.; Chege, B.; Nyamota, R.; Mutiiria, M.; Maina, J.; Thumbi, S. M.; Nyamai, M.; Kahariri, S.; Sitawa, R.; Kimutai, J.; Kuria, W.; Mwatondo, A.; Bett, B. Serological Evidence of Single and Mixed Infections of Rift Valley Fever Virus, Brucella Spp. And Coxiella Burnetii in Dromedary Camels in Kenya. *PLoS Neglected Trop. Dis.* **2021**, *15*, No. e0009275.

(6) Shome, R.; Kalleshamurthy, T.; Nagaraj, C.; Rathore, Y.; Ramanjinappa, K. D.; Skariah, S.; Mohandoss, N.; Shome, B. R.; Chanda, M. M.; Hemadri, D. Countrywide Cross-Sectional Study of Swine Brucellosis Sero-Prevalence in Indian Subcontinent during 2018−2019. *Trop. Anim. Health Prod.* **2022**, *54*, 114.

(7) Zhang, T.; Liang, X.; Zhu, X.; Sun, H.; Zhang, S. An Outbreak of Brucellosis via Air-Born Transmission in a Kitchen Wastes Disposing Company in Lianyungang, China. *Int. J. Infect. Dis.* **2020**, *96*, 39−41.

(8) Yagupsky, P.; Morat, P.; Colmenero, J. D. Laboratory Diagnosis of Human Brucellosis. *Clin. Microbiol. Rev.* **2020**, *33*, e00073−e00019.

(9) Jiang, H.; O'Callaghan, D.; Ding, J. B. Brucellosis in China: History, Progress and Challenge. *Infect. Dis. Poverty* **2020**, *9*, 55.

(10) De Miguel, M. J.; Marín, C. M.; Muñoz, P. M.; Dieste, L.; Grilló, M. J.; Blasco, J. M. Development of a Selective Culture Medium for Primary Isolation of the Main Brucella Species. *J. Clin. Microbiol.* **2011**, *49*, 1458−1463.

(11) Di Bonaventura, G.; Angeletti, S.; Ianni, A.; Petitti, T.; Gherardi, G. Microbiological Laboratory Diagnosis of Human Brucellosis: An Overview. *Pathogens* **2021**, *10*, 1623.

(12) Yin, D.; Bai, Q.; Wu, X.; Li, H.; Shao, J.; Sun, M.; Jiang, H.; Zhang, J. Paper-Based Elisa Diagnosis Technology for Human Brucellosis Based on a Multiepitope Fusion Protein. *PLoS Negl.ected Trop. Dis.* **2021**, *15*, No. e0009695.

(13) Dong, S. B.; Xiao, D.; Liu, J. Y.; Bi, H. M.; Zheng, Z. R.; Da Wang, L.; Yang, X. W.; Tian, G. Z.; Zhao, H. Y.; Piao, D. R.; Xing, Z. F.; Jiang, H. Fluorescence Polarization Assay Improves the Rapid Detection of Human Brucellosis in China. *Infect. Dis. Poverty* **2021**, *10*, 46.

(14) Camacho-Martínez, J. C.; Rios-Lugo, M. J.; Gaytán-Hernández, D.; Hernández-Mendoza, H. Comparison of a Brucella Enzyme Immunoassay and the Standard Agglutination with 2-Mercaptoethanol Test in the Diagnosis and Monitoring of Brucellosis in Mexican Patients. *Clin. Lab.* **2020**, *66*, No. 190932.

(15) Cernyseva, M. I.; Knjazeva, E. N.; Egorova, L. S. Study of the Plate Agglutination Test with Rose Bengal Antigen for the Diagnosis of Human Brucellosis. *Bull. W. H. O.* **1977**, *55*, 669−674.

(16) Yang, X.; Wang, Y.; Liu, Y.; Huang, J.; Tan, Q.; Ying, X.; Hu, Y.; Li, S. A Label-Based Polymer Nanoparticles Biosensor Combined with Loop-Mediated Isothermal Amplification for Rapid, Sensitive, and Highly Specific Identification of Brucella Abortus. *Front. Bioeng. Biotechnol.* **2021**, *9*, No. 758564.

(17) He Che, L.; Qi, C.; Guo Bao, W.; Feng Ji, X.; Liu, J.; Du, N.; Gao, L.; Yu Zhang, K.; Xiang Li, Y. Monitoring the Course of Brucella Infection with QPCR-Based Detection. *Int. J. Infect. Dis.* **2019**, *89*, 66−71.

(18) Trotta, A.; Marinaro, M.; Cirilli, M.; Sposato, A.; Adone, R.; Beverelli, M.; Buonavoglia, D.; Corrente, M. Brucella Melitensis B115-Based ELISA to Unravel False Positive Serologic Reactions in Bovine Brucellosis: A Field Study. *BMC Vet. Res.* **2020**, *16*, 50.

(19) Patra, K. P.; Saito, M.; Atluri, V. L.; Rolán, H. G.; Young, B.; Kerrinnes, T.; Smits, H.; Ricaldi, J. N.; Gotuzzo, E.; Gilman, R. H.; Tsolis, R. M.; Vinetz, J. M. A Protein-Conjugate Approach to Develop a Monoclonal Antibody-Based Antigen Detection Test for the Diagnosis of Human Brucellosis. *PLoS Neglected Trop. Dis.* **2014**, *8*, No. e2926.

(20) Ahmed, I. M.; Khairani-Bejo, S.; Hassan, L.; Bahaman, A. R.; Omar, A. R. Serological Diagnostic Potential of Recombinant Outer Membrane Proteins (ROMPs) from Brucella Melitensis in Mouse Model Using Indirect Enzyme-Linked Immunosorbent Assay. *BMC Vet. Res.* **2015**, *11*, 275.

(21) Corrente, M.; Desario, C.; Parisi, A.; Grandolfo, E.; Scaltrito, D.; Vesco, G.; Colao, V.; Buonavoglia, D. Serological Diagnosis of Bovine Brucellosis Using B. Melitensis Strain B115. *J. Microbiol. Methods* **2015**, *119*, 106−109.

(22) Çiftci, A.; İça, T.; Savaşan, S.; Sareyyüpoğlu, B.; Akan, M.; Diker, K. S. Evaluation of PCR Methods for Detection of Brucella Strains from Culture and Tissues. *Trop. Anim. Health Prod.* **2017**, *49*, 755−763.

(23) Mirnejad, R.; Doust, R. H.; Kachuei, R.; Mortazavi, S. M.; Khoobdel, M.; Ahamadi, A. Simultaneous Detection and Differentiates of Brucella Abortus and Brucella Melitensis by Combinatorial PCR. *Asian Pac. J. Trop. Med.* **2012**, *5*, 24−28.
(24) Zhu, M.; Zhang, J.; Cao, J.; Ma, J.; Li, X.; Shi, F. Ultrasensitive Dual-Color Rapid Lateral Flow Immunoassay via Gold Nanoparticles with Two Different Morphologies for the Serodiagnosis of Human Brucellosis. *Anal. Bioanal. Chem.* **2019**, *411*, 8033−8042.
(25) Shi, F.; Tang, Y.; Xu, Z. H.; Sun, Y. X.; Ma, M. Z.; Chen, C. F. Visual Typing Detection of Brucellosis with a Lateral Flow Immunoassay Based on Coloured Latex Microspheres. *J. Appl. Microbiol.* **2022**, *132*, 199−208.
(26) Lu, J.; Wu, Z.; Liu, B.; Wang, C.; Wang, Q.; Zhang, L.; Wang, Z.; Chen, C.; Fu, Y.; Li, C.; Li, T. A Time-Resolved Fluorescence Lateral Flow Immunoassay for Rapid and Quantitative Serodiagnosis of Brucella Infection in Humans. *J. Pharm. Biomed. Anal.* **2021**, *200*, No. 114071.
(27) (27) Saha, D.; Roy, D.; Dhar, T. K. Immunofiltration Assay for Aflatoxin B1 Based on the Separation of Pre-Immune Complexes. *J. Immunol. Methods* **2013**, *392*, 24−28.
(28) Zhang, P.; Bao, Y.; Draz, M. S.; Lu, H.; Liu, C.; Han, H. Rapid and Quantitative Detection of C-Reactive Protein Based on Quantum Dots and Immunofiltration Assay. *Int. J. Nanomed.* **2015**, *10*, 6161−6173.
(29) Jia, M.; Liu, J.; Zhang, J.; Zhang, H. An Immunofiltration Strip Method Based on the Photothermal Effect of Gold Nanoparticles for the Detection of: Escherichia Coli O157:H7. *Analyst* **2019**, *144*, 573−578.
(30) Shi, F.; Sun, Y.; Wu, Y.; Zhu, M.; Feng, D.; Zhang, R.; Peng, L.; Chen, C. A Novel, Rapid and Simple Method for Detecting Brucellosis Based on Rapid Vertical Flow Technology. *J. Appl. Microbiol.* **2020**, *128*, 794−802.
(31) Zhang, R.; Yan, X.; Fan, K. Nanozymes Inspired by Natural Enzymes. *Acc. Mater. Res.* **2021**, *2*, 534−547.
(32) Tang, G.; He, J.; Liu, J.; Yan, X.; Fan, K. Nanozyme for Tumor Therapy: Surface Modification Matters. *Exploration* **2021**, *1*, No. 75.
(33) Wang, Z.; Zhao, Y.; Hou, Y.; Tang, G.; Zhang, R.; Yang, Y.; Yan, X.; Fan, K. A Thrombin-Activated Peptide-Templated Nanozyme for Remedying Ischemic Stroke via Thrombolytic and Neuroprotective Actions. *Adv. Mater.* **2023**, No. e2210144.
(34) Gao, Z.; Xu, M.; Lu, M.; Chen, G.; Tang, D. Urchin-like (Gold Core)@(Platinum Shell) Nanohybrids: A Highly Efficient Peroxidase-Mimetic System for in Situ Amplified Colorimetric Immunoassay. *Biosens. Bioelectron.* **2015**, *70*, 194−201.
(35) (35) Panferov, V. G.; Safenkova, I. V.; Zherdev, A. V.; Dzantiev, B. B. The Steadfast Au@Pt Soldier: Peroxide-Tolerant Nanozyme for Signal Enhancement in Lateral Flow Immunoassay of Peroxidase-Containing Samples. *Talanta* **2021**, *225*, No. 121961.
(36) Loynachan, C. N.; Thomas, M. R.; Gray, E. R.; Richards, D. A.; Kim, J.; Miller, B. S.; Brookes, J. C.; Agarwal, S.; Chudasama, V.; McKendry, R. A.; Stevens, M. M. Platinum Nanocatalyst Amplification: Redefining the Gold Standard for Lateral Flow Immunoassays with Ultrabroad Dynamic Range. *ACS Nano* **2018**, *12*, 279−288.
(37) Jiang, T.; Song, Y.; Wei, T.; Li, H.; Du, D.; Zhu, M. J.; Lin, Y. Sensitive Detection of Escherichia Coli O157:H7 Using Pt-Au Bimetal Nanoparticles with Peroxidase-like Amplification. *Biosens. Bioelectron.* **2016**, *77*, 687−694.
(38) Gao, Z.; Ye, H.; Tang, D.; Tao, J.; Habibi, S.; Minerick, A.; Tang, D.; Xia, X. Platinum-Decorated Gold Nanoparticles with Dual Functionalities for Ultrasensitive Colorimetric in Vitro Diagnostics. *Nano Lett.* **2017**, *17*, 5572−5579.
(39) McKee, D. W. Catalytic Decomposition of Hydrogen Peroxide by Metals and Alloys of the Platinum Group. *J. Catal.* **1969**, *14*, 355.
(40) Liu, B.; Wu, Z.; Liang, C.; Lu, J.; Li, J.; Zhang, L.; Li, T.; Zhao, W.; Fu, Y.; Hou, S.; Tang, X.; Li, C. Development of a Smartphone-Based Nanozyme-Linked Immunosorbent Assay for Quantitative Detection of SARS-CoV-2 Nucleocapsid Phosphoprotein in Blood. *Front. Microbiol.* **2021**, *12*, No. 692831.
(41) Liang, C.; Liu, B.; Li, J.; Lu, J.; Zhang, E.; Deng, Q.; Zhang, L.; Chen, R.; Fu, Y.; Li, C.; Li, T. A Nanoenzyme Linked Immunochromatographic Sensor for Rapid and Quantitative Detection of SARS-CoV-2 Nucleocapsid Protein in Human Blood. *Sens. Actuators, B* **2021**, *349*, No. 130718.
(42) Wang, X.; Quinn, P. J. Lipopolysaccharide: Biosynthetic Pathway and Structure Modification. *Prog. Lipid Res.* **2010**, *49*, 97−107.
(43) Whitfield, C.; Williams, D. M.; Kelly, S. D. Lipopolysaccharide O-Antigens-Bacterial Glycans Made to Measure. *J. Biol. Chem.* **2020**, *295*, 10593−10609.
(44) Liu, B.; Knirel, Y. A.; Feng, L.; Perepelov, A. V.; Senchenkova, S.' N.; Reeves, P. R.; Wang, L. Structural Diversity in Salmonella O Antigens and Its Genetic Basis. *FEMS Microbiol. Rev.* **2014**, *38*, 56−89.
(45) Liu, B.; Furevi, A.; Perepelov, A. V.; Guo, X.; Cao, H.; Wang, Q.; Reeves, P. R.; Knirel, Y. A.; Wang, L.; Widmalm, G. Structure and Genetics of Escherichia Coli O Antigens. *FEMS Microbiol. Rev.* **2020**, *44*, 655−683.
(46) Bonfini, B.; Chiarenza, G.; Paci, V.; Sacchini, F.; Salini, R.; Vesco, G.; Villari, S.; Zilli, K.; Tittarelli, M. Cross-reactivity in Serological Tests for Brucellosis: A Comparison of Immune Response of Escherichia Coli O157:H7 and Yersinia Enterocolitica o:9 vs Brucella Spp. *Vet. Ital.* **2018**, *54*, 107−114.
(47) Fang, A.; Sun, Y.; Feng, D.; Ma, M.; Xu, Z.; Zhang, T.; Shi, F. Flower-like Gold Nanoparticles Labeled and Silver Deposition Rapid Vertical Flow Technology for Highly Sensitive Detection of: Brucella Antibodies. *Analyst* **2021**, *146*, 5362−5368.
(48) Fang, A.; Feng, D.; Luo, X.; Shi, F. Gold Nanoparticles Prepared with Cyclodextrin Applied to Rapid Vertical Flow Technology for the Detection of Brucellosis. *Biosensors* **2022**, *12*, 531.
(49) Ge, L.; Wang, D.; Lian, F.; Zhao, J.; Wang, Y.; Zhao, Y.; Zhang, L.; Wang, J.; Song, X.; Li, J.; Xu, K. Lateral Flow Immunoassay for Visible Detection of Human Brucellosis Based on Blue Silica Nanoparticles. *Front. Vet. Sci.* **2021**, *8*, No. 771341.

https://doi.org/10.1021/acsomega.3c03381
ACS Omega 2023, 8, 29534−29542